Synchronous Motor Observability Study and a New Robust MRAS Speed Observer with an Improved Zero-speed Position Estimation Design for Surface PMSM

DALILA ZALTNI[1,2] and MOHAMED NACEUR ABDELKRIM[1]
[1]Ecole Nationale d'Ingénieurs de Gabès
Unité de Recherche Modélisation, Analyse et Commande des Systèmes
Rue Omar al Khattab, Zrig, 6029 Gabès
TUNISIA
[2]Ecole Nationale Supérieure de l'Electroniques et ses Applications
Equipe Commande des Systèmes
6, Avenue du Ponceau, 95014, Cergy-Pontoise
FRANCE
dalila.zaltni@ensea.fr

Abstract: This paper deals with the Permanent Magnet Synchronous Motor (PMSM) observability problems and proposes a simple and effective solution to improve the rotor speed and position estimation for Surface PMSM (SPMSM). In fact, the problem of loss of observability at low frequency range is always recognized in experimental settings. Nevertheless, there are no sufficient theoretical observability analyses for the PMSM. In the literature, only the sufficient observability condition has been presented. Therefore, the current work is aimed specially to the necessary observability condition analysis. In order to improve the rotor speed and position estimation in the case of SPMSM, a special attention is given to Model Reference Adaptive System (MRAS). MRAS based techniques are one of the best methods to estimate the rotor speed and position due to its performances and straight forward stability approach. In this paper, we propose a new robust MRAS scheme based on sliding mode techniques to estimate the rotor speed of a SPMSM. Furthermore, an Estimator/Observer swapping system is designed to overcome position observability problems at zero speed which is an unobservable state point. The stability of the proposed MRAS observer is also presented and discussed. Various tests are carried out in simulation using MATLAB/SIMULINK to illustrate the obtained theoretical results.

Key–Words: Permanent magnet synchronous motor, Observability analysis, Model reference adaptive system, Observer, Sliding mode

1 Introduction

Industries concerned by PMSMs are continuously seeking for cost reductions in their products. These reductions often impose the minimization of number of sensors used for control purposes because they substantially contribute to increase the complexity and cost of the full installation (additional cables, maintenance, etc.) and the default probability. This imposes the use of observers in order to realize sensor-less control design. Since many observers for PMSM sensorless control are available, as the extended Kalman filter [1], the full order and the reduced order observers [2], the LMI based methods [3], the high-frequency signal injection methods [4,5], the sliding mode observers [6,7] and so on, the main research stream has been focused on searching for reliable speed and position estimation methods with the aim to replace the mechanical sensors with the observer in the control system [8-11]. However, the current problems to successfully apply sensor-less control for PMSM are the existence of operating regimes for which the observer performances are remarkably deteriorated due to the difficulties in estimating correctly the motor position. The failure of sensor-less schemes in some particular operating conditions has been always recognized in experimental setting. In the case of induction motors, the observability has been studied by many authors [12,13]. Nevertheless, there are no sufficient theoretical observability studies for the PMSM. Only the sufficient observability condition has been presented in literature. For instance, in [14], observability is analyzed in the case of constant high speed operation. In [15] and [16], the author gives only the sufficient observability condition (not necessary) of the PMSM in the particular case of constant speed. The current

work is aimed specially to the necessary observability condition analysis. In [17] and [18], we have given the sufficient condition of loss of observability for the SPMSM. In this paper, observability of both the Interior PMSM (IPMSM) and the SPMSM is studied and discussed at different operating conditions then the necessary and sufficient observability condition is presented.

In order to illustrate the observability problems shown in the case of SPMSM and try to find solutions, an observer should be designed. In a sensor-less PMSM, the speed can be estimated by various techniques. A speed estimate can be directly obtained using the machine's model equations. However, the accuracy is not very good. Other techniques are available: the Extended Kalman Filter method and the Luenberger observer construct full order estimators based on the machine model. Both approaches tend to depend heavily on the machine parameters and are generally difficult to implement. Compared with other methods, MRAS based techniques are one of the best methods to estimate the rotor speed due to its performance and straight forward stability approach. The MRAS system is well-known in the sensor-less control of Induction Motors and has been proved to be effective and physically clear [19, 20, 21]. However, MRAS techniques using conventional PI controllers still sensible to parameter variations [22, 23]. To overcome this problem, sliding mode techniques can be introduced to the MRAS structure to ensure robustness and accuracy of the observer. In this paper, we propose a new robust MRAS structure based on sliding mode techniques [24] which have attractive advantages of robustness to disturbances and insensitivity to parameter variations when the sliding mode happens [25, 26, 27]. The reference model used in the proposed MRAS system is a Second Order Sliding Mode (SOSM) observer. This reference model is a speed-independent observer which computes the estimated Back Electro-Motive Forces (BEMFs). The proposed model reference based on Higher Order Sliding Mode (HOSM) techniques is designed in order to ensure the robustness of the observer and to reduce the chattering phenomenon [28, 29, 30, 31]. Therefore, the output signals of the reference model are smooth enough to be used directly as reference BEMFs. A speed-dependent model is designed as adjustable model which computes the estimated BEMFs. Outputs of the reference and the adjustable model are then fed into an adaptive sliding mode mechanism ensuring the convergence of the estimated speed to the real speed. The proposed MRAS observer is of high robustness and accuracy compared to other MRAS based techniques presented in the literature. The stability of the designed observer is presented and discussed. The rotor position is obtained from the phase of the estimated BEMFs. Since the position can not be calculated at very low frequencies, because the BEMFs are practically non existent, an Estimator/Observer swapping system is proposed to ensure rotor position estimation in all frequencies range. Tests are carried out at various operating conditions to illustrate the effectiveness and the high robustness of the proposed estimation design.

This paper is organized as follows: In section two, the mathematical model of both IPMSM and SPMSM are presented. In section three, the nonlinear observability is recalled. Observability analysis of both IPMSM and SPMSM is presented is section four. The proposed robust MRAS speed observer based sliding mode techniques is given in section five. Simulation results are illustrated in section six. Finally, some concluding remarks are drawn in the last section.

2 Synchronous Motor Models

2.1 Interior Permanent Magnet Case

The mathematical model of the IPMSM in the (d-q) rotating coordinate is given by equations (1) and (2) [32].

$$\begin{pmatrix} \frac{di_d}{dt} \\ \frac{di_q}{dt} \end{pmatrix} = \begin{pmatrix} -\frac{R}{L_d} & \frac{L_q}{L_d}P\omega \\ -\frac{L_d}{L_q}P\omega & -\frac{R}{L_q} \end{pmatrix} \begin{pmatrix} i_d \\ i_q \end{pmatrix} + \begin{pmatrix} \frac{1}{L_d} & 0 \\ 0 & \frac{1}{L_q} \end{pmatrix} \begin{pmatrix} u_d \\ u_q \end{pmatrix} + \begin{pmatrix} 0 \\ \frac{-P\phi_m}{L_q}\omega \end{pmatrix} \quad (1)$$

$$\frac{d\omega}{dt} = \frac{P}{J}[(L_d - L_q)i_d + \phi_m]i_q - \frac{f_v}{J}\omega - \frac{T_l}{J} \quad (2)$$

where
ω is the rotor speed.
R is the stator resistance.
L_d, L_q are the (d-q) stator inductance components.
P is the pair pole number.
J is the moment of inertia.
ϕ_m is the rotor flux.
f_v is the viscous friction.
T_l is the load torque.
$[i_d \quad i_q]^T$, $[u_d \quad u_q]^T$ are the (d-q) stator current and voltage vector respectively.
Transforming the model given by (1) on the (α, β)

fixed coordinate, (3) is derived [32]:

$$\begin{pmatrix} u_\alpha \\ u_\beta \end{pmatrix} = \begin{pmatrix} R+sL_\alpha & sL_{\alpha\beta} \\ sL_{\alpha\beta} & R+sL_\beta \end{pmatrix} \begin{pmatrix} i_\alpha \\ i_\beta \end{pmatrix} + \omega_e K_e \begin{pmatrix} -\sin(\theta_e) \\ \cos(\theta_e) \end{pmatrix} \quad (3)$$

where
$L_\alpha = L_0 + L_1 cos(2\theta_e)$
$L_\beta = L_0 - L_1 cos(2\theta_e)$
$L_{\alpha\beta} = L_1 \sin(2\theta_e)$
$L_0 = \frac{L_d+L_q}{2}$
$L_1 = \frac{L_d-L_q}{2}$
$\omega_e = P.\omega$ is the electric rotor speed.
s is the differential operator.
K_e is the BEMF constant.
The used inverse Park's transformation is:

$$\begin{pmatrix} x_\alpha \\ x_\beta \end{pmatrix} = \begin{pmatrix} \cos(\theta_e) & -\sin(\theta_e) \\ \sin(\theta_e) & \cos(\theta_e) \end{pmatrix} \begin{pmatrix} x_d \\ x_q \end{pmatrix} \quad (4)$$

With L_0 and L_1 terms, the equation system (3) becomes:

$$\begin{aligned} \begin{pmatrix} u_\alpha \\ u_\beta \end{pmatrix} &= R \begin{pmatrix} i_\alpha \\ i_\beta \end{pmatrix} + sL_0 \begin{pmatrix} i_\alpha \\ i_\beta \end{pmatrix} \\ &+ \omega_e K_e \begin{pmatrix} -\sin(\theta_e) \\ \cos(\theta_e) \end{pmatrix} \\ &+ L_1 \omega_e \begin{pmatrix} -2\sin(2\theta_e) & 2\cos(2\theta_e) \\ 2\cos(2\theta_e) & 2\sin(2\theta_e) \end{pmatrix} \begin{pmatrix} i_\alpha \\ i_\beta \end{pmatrix} \\ &+ L_1 \begin{pmatrix} \cos(2\theta_e) & \sin(2\theta_e) \\ \sin(2\theta_e) & -\cos(2\theta_e) \end{pmatrix} s \begin{pmatrix} i_\alpha \\ i_\beta \end{pmatrix} \end{aligned} \quad (5)$$

Therefore, the dynamic model of the IPMSM in the (α, β) fixed coordinate is given by equation (6) and (7):

$$\begin{pmatrix} \dot{i}_\alpha \\ \dot{i}_\beta \end{pmatrix} = \Gamma^{-1} \left[\begin{pmatrix} u_\alpha \\ u_\beta \end{pmatrix} - \begin{pmatrix} R - 2L_1\omega_e \sin(2\theta_e) & 2L_1\omega_e \cos(2\theta_e) \\ 2L_1\omega_e \cos(2\theta_e) & R + 2L_1\omega_e \sin(2\theta_e) \end{pmatrix} \begin{pmatrix} i_\alpha \\ i_\beta \end{pmatrix} - \omega_e K_e \begin{pmatrix} -\sin(\theta_e) \\ \cos(\theta_e) \end{pmatrix} \right] \quad (6)$$

$$\begin{aligned} \dot{\omega}_e &= \frac{P}{J}[2L_1(cos(\theta_e)i_\alpha + sin(\theta_e)i_\beta) + \phi_m](-sin(\theta_e)i_\alpha \\ &+ cos(\theta_e)i_\beta) - \frac{f_v}{J}\omega_e - \frac{T_l}{J} \end{aligned} \quad (7)$$

where $\Gamma^{-1} = \frac{1}{L_0^2 - L_1^2}$
$\times \begin{pmatrix} L_0 - L_1\cos(2\theta_e) & -L_1 sin(2\theta_e) \\ -L_1 sin(2\theta_e) & L_0 + L_1\cos(2\theta_e) \end{pmatrix}$

2.2 Surface Mounted Permanent Magnet Case

In the SPMSM we have $L_d = L_q$ then $L_1 = 0$.
Thus, from equation (6) and (7), we can deduce the dynamic model of the SPMSM:

$$\begin{pmatrix} \dot{i}_\alpha \\ \dot{i}_\beta \end{pmatrix} = \frac{1}{L_0} \left[\begin{pmatrix} u_\alpha \\ u_\beta \end{pmatrix} - R \begin{pmatrix} i_\alpha \\ i_\beta \end{pmatrix} - \omega_e K_e \begin{pmatrix} -\sin(\theta_e) \\ \cos(\theta_e) \end{pmatrix} \right] \quad (8)$$

$$\begin{aligned} \dot{\omega}_e &= \frac{P}{J}\phi_m(-sin(\theta_e)i_\alpha + cos(\theta_e)i_\beta) - \frac{f_v}{J}\omega_e \\ &- \frac{T_l}{J} \end{aligned} \quad (9)$$

3 Nonlinear Observability

In this section, the nonlinear observability is recalled [33]. We consider systems of the form:

$$\sum : \begin{cases} \dot{x} = f(x,u) \\ y = h(x) \end{cases} \quad (10)$$

Where $x \in X \subset R^n$ is the state vector, $u \in U \subset R^m$ is the control vector, $y \in R^p$ is the output vector, f and h are C^∞ functions.

Definition 3-1(Indistinguishability and observability)
Consider the system $\sum$ and let x_0 and x_1 be two points of the state space X.
The pair x_0 and x_1 are indistinguishable (denoted $x_0 I x_1$) if ($\sum$,x_0) and ($\sum$,x_1) realize the same input-output map, i.e., for every admissible input $(u(t), [t_0 \quad t_1])$

$$\sum_{x_0}(u(t),[t_0,t_1]) = \sum_{x_1}(u(t),[t_0,t_1])$$

Indistinguishability I is an equivalence relation on X. $\sum$ is said to be observable at x_0 if $I(x_0) = x_0$ and $\sum$ is observable if $I(x) = x$ for every $x \in X$.

Definition 3-2(Locally weak observability)
Consider the system $\sum$ and let x_0 be a point of the state space X.

- $\sum$ is locally weakly observable at x_0 if there exist an open neighborhood V of x_0 such that for every open neighborhood v of x_0 contained in V, $I_v(x_0) = x_0$ and is locally weakly observable if it's so at every $x \in X$.

- $\sum$ is locally regularly weakly observable at x_0 if it is locally weakly observable at x_0 and the $n-1$ derivatives outputs are sufficient to locally observe the system.

Now in order to recall the well known rank criterion, the following Lie-B*ä*cklund derivative is presented:

According to system (10), we denote by

$$\begin{cases} L_f h &= \dfrac{\partial h}{\partial x} f \\ L_f^2 h &= \dfrac{\partial L_f h}{\partial x} f + \dfrac{\partial L_f h}{\partial u}\dot{u} \\ L_f^3 h &= \dfrac{\partial L_f^2 h}{\partial x} f + \dfrac{\partial L_f^2 h}{\partial u}\dot{u} + \dfrac{\partial L_f^2 h}{\partial \dot{u}}\ddot{u} \\ \vdots & \\ L_f^p h &= \dfrac{\partial L_f^{p-1} h}{\partial x} f + \sum_{i=1}^{p-2} \dfrac{\partial L_f^{p-1} h}{\partial u^{(i-1)}} u^{(i)} \end{cases}$$

where $u^{(i)}$ is the i^{th} derivative of u.

Rank Criterion
A sufficient locally regularly weakly observable condition at x_0 of (10) is that there exists $(u,\dot{u},...,)$ such that:

$$rank(J)\mid_{x_0} = rank \begin{pmatrix} dh \\ dL_f h \\ dL_f^2 h \\ . \\ . \\ . \\ dL_f^{n-1} h \end{pmatrix} \mid_{x_0} = n \qquad (11)$$

Remark 3-1

1. The notion of locally regularly weakly observability is introduced in order to design an observer of dimension equal to *n*.

2. The condition (11) depends on $(u,\dot{u},...)$ and this is an implicit justification of the universal inputs introduced in [34].

4 Observability Study of the PMSM

To determine conditions under which it is possible to compute rotor speed and position information from measured output, let's consider the state vector $x = [i_\alpha, \quad i_\beta, \quad \theta_e, \quad \omega_e]^T$ and the output vector $y = [i_\alpha, \quad i_\beta]^T$. Voltages and currents are assumed to be measurable. The order of the state vector of the PMSM is $n = 4$. Thus, according to the observability rank criterion mentioned earlier, the PMSM is locally regularly weakly observable at x_0 for $(u,\dot{u},...)$ if the following condition is fulfilled:

$$rank(J)|_{x_0,(u,\dot{u},...)} = 4 \qquad (12)$$

4.1 Observability analysis of the IPMSM

Consider the system (6) and (7) as:

$$\begin{pmatrix} \dot{x}_1 \\ \dot{x}_2 \\ \dot{x}_3 \\ \dot{x}_4 \end{pmatrix} = \frac{1}{L_0^2 - L_1^2} \begin{pmatrix} \Lambda_{11}\gamma_1 + \Lambda_{12}\gamma_2 \\ \Lambda_{21}\gamma_1 + \Lambda_{22}\gamma_2 \\ x_4 \\ T_e - m x_4 - \tau \end{pmatrix} \qquad (13)$$

Where

$$\Lambda = \begin{pmatrix} L_0 - L_1\cos(2\theta) & -L_1 sin(2\theta) \\ -L_1 sin(2\theta) & L_0 + L_1\cos(2\theta) \end{pmatrix}$$

Λ_{ij} is the i^{th} row of the j^{th} column of the matrix Λ
$\gamma_1 = v_\alpha - (R - 2L_1 x_4 \sin(2x_3))x_1 + 2L_1 x_4 \cos(2x_3)x_2 + x_4 K_e sin(x_3)$
$\gamma_2 = v_\beta - (R - 2L_1 x_4 \sin(2x_3))x_2 - 2L_1 x_4 \cos(2x_3)x_1 - x_4 K_e cos(x_3)$
$T_e = \frac{P}{J}[2L_1(cos(x_3)x_1 + sin(x_3)x_2) + \phi_m](-sin(x_3)x_1 + cos(x_3)x_2)$ is the electromagnetic torque. Let

$$f(x) = \frac{1}{L_0^2 - L_1^2} \begin{pmatrix} \Lambda_{11}\gamma_1 + \Lambda_{12}\gamma_2 \\ \Lambda_{21}\gamma_1 + \Lambda_{22}\gamma_2 \\ x_4 \\ T_e - m x_4 - \tau \end{pmatrix}$$

and $h(x) = y$.

Then, look at the vector of information generated from the output and its only first derivatives:

$$O_1 = \begin{pmatrix} h_1 \\ h_2 \\ L_f h_1 \\ L_f h_2 \end{pmatrix} \qquad (14)$$

The associated observability matrix is:

$$J_1 = \frac{\partial}{\partial x} O_1 \qquad (15)$$

This gives:

$$J_1 = \begin{pmatrix} 1 & 0 & 0 & 0 \\ 0 & 1 & 0 & 0 \\ \frac{\partial L_f^1 h_1}{\partial x_1} & \frac{\partial L_f^1 h_1}{\partial x_2} & \frac{\partial L_f^1 h_1}{\partial x_3} & \frac{\partial L_f^1 h_1}{\partial x_4} \\ \frac{\partial L_f^1 h_2}{\partial x_1} & \frac{\partial L_f^1 h_2}{\partial x_2} & \frac{\partial L_f^1 h_2}{\partial x_3} & \frac{\partial L_f^1 h_2}{\partial x_4} \end{pmatrix} \quad (16)$$

The computation of the corresponding determinant gives:

$$\Delta_1 = \frac{\partial L_f^1 h_1}{\partial x_3}.\frac{\partial L_f^1 h_2}{\partial x_4} - \frac{\partial L_f^1 h_2}{\partial x_3}.\frac{\partial L_f^1 h_1}{\partial x_4} \quad (17)$$

The previous equation leads to:

$$\begin{aligned} \Delta_1 &= [[2L_1\sin(2x_3)\gamma_1 + (L_0 - L_1\cos(2x_3))\frac{\partial \gamma_1}{\partial x_3} \\ &- 2L_1\cos(2x_3)\gamma_2 \\ &- L_1\sin(2x_3)\frac{\partial \gamma_2}{\partial x_3}].[-L_1\sin(2x_3)\frac{\partial \gamma_1}{\partial x_4} \\ &+ (L_0 + L_1\cos(2x_3))\frac{\partial \gamma_2}{\partial x_4}] - [-2L_1\cos(2x_3)\gamma_1 \\ &- L_1 sin(2x_3)\frac{\partial \gamma_1}{\partial x_3} - 2L_1\sin(2x_3)\gamma_2 \\ &+ (L_0 - L_1\cos(2x_3))\frac{\partial \gamma_2}{\partial x_3}][(L_0 - L_1\cos(2x_3))\frac{\partial \gamma_1}{\partial x_4} \\ &- L_1\sin(2x_3)\frac{\partial \gamma_2}{\partial x_4}]]/(L_0^2 - L_1^2) \end{aligned} \quad (18)$$

where

$$\begin{aligned} \frac{\partial \gamma_1}{\partial x_3} &= 4L_1x_4(\cos(2x_3)x_1 - \sin(2x_3)x_2) + x_4K_e\cos(x_3) \\ \frac{\partial \gamma_2}{\partial x_3} &= 4L_1x_4(\sin(2x_3)x_1 - \cos(2x_3)x_2) + x_4K_e\sin(x_3) \\ \frac{\partial \gamma_1}{\partial x_4} &= 2L_1(\sin(2x_3)x_1 + \cos(2x_3)x_2) + K_e\sin(x_3) \\ \frac{\partial \gamma_2}{\partial x_4} &= -2L_1(\cos(2x_3)x_1 - \sin(2x_3)x_2) - K_e\cos(x_3) \end{aligned}$$

Case 1: IPMSM at zero speed

It is important to note that for interior permanent magnet synchronous motor L_1 is always different from 0, consequently the J_1 determinant at zero speed ($x_4 = 0$) is:

$$\begin{aligned} \Delta_1 &= [[2L_1\sin(2x_3)(u_\alpha - Rx_1) - 2L_1\cos(2x_3)(u_\beta \\ &- Rx_2)].[-L_1\sin(2x_3)(2L_1\sin(2x_3)x_1 \\ &+ 2L_1\cos(2x_3)x_2 + K_e\sin(x_3)) + (L_0 \\ &+ L_1\cos(2x_3))(-2L_1\cos(2x_3)x_1 \\ &- 2L_1\sin(2x_3)x_2 - K_e\cos(x_3))]]/(L_0^2 - L_1^2) \end{aligned} \quad (19)$$

Remark 4-1

Looking at the previous expression (19), we remark that at zero speed operation Δ_1 depends on current and voltage. Therefore, we have always the opportunity to find again the observability property by injection of a continue current. Thus, we can conclude that the IPMSM is always observable.

4.2 Observability analysis of the SPMSM

In this section, we present the observability analysis of the SPMSM and we give a sufficient condition of loss of the observability property.

In this case, we have $L_d = L_q$ then $L_1 = 0$. Therefore, the expression of determinant of J_1 given in (18) becomes:

$$\Delta_1 = -K_e^2 x_4 \quad (20)$$

Remark 4-2

The determinant Δ_1 is dependent only on x_4. Thus, for the considered output and only its first derivative the SPMSM is locally weakly observable at x_0 if $x_4 \neq 0$. This condition is independent on the considered input $u_{\alpha,\beta}$.

Now the question is to look if higher derivatives of output overcome the observability singularity at zero speed $x_4 = 0$.

For that, let's consider the model of the SPMSM given by equations (8) and (9) in the form of (10) where

$$f(x,u) = \begin{pmatrix} ax_1 + bx_4 sin(x_3) + cu_\alpha \\ ax_2 - bx_4 cos(x_3) + cu_\beta \\ x_4 \\ k_t(-sin(x_3)x_1 + cos(x_3)x_2) - mx_4 - \tau \end{pmatrix}$$

and $h(x) = [x_1, x_2]^T$, with $a = \frac{-R}{L_0}$, $b = \frac{K_e}{L_0}$, $c = \frac{1}{L_0}$, $k_t = \frac{p\phi_m}{J}$, $m = \frac{f_v}{J}$ and $\tau = \frac{T_l}{J}$.

Let's look to the following vector of information generated from:

$$O_2 = \begin{pmatrix} h_1 \\ h_2 \\ L_f h_1 \\ L_f h_2 \\ L_f^2 h_1 \\ L_f^2 h_2 \end{pmatrix} \quad (21)$$

The associated observability matrix is:

$$J_2 = \frac{\partial}{\partial x} O_2 \quad (22)$$

Condition (12) can be tested by searching for a regular

matrix constructed from any four rows of matrix J_2. Let's consider only the 1^{st}, 2^{nd}, 5^{th} and the 6^{th} rows of J_2 as.

$$J_2 = \begin{pmatrix} 1 & 0 & 0 & 0 \\ 0 & 1 & 0 & 0 \\ \frac{\partial L_f^2 h_1}{\partial x_1} & \frac{\partial L_f^2 h_1}{\partial x_2} & \frac{\partial L_f^2 h_1}{\partial x_3} & \frac{\partial L_f^2 h_1}{\partial x_4} \\ \frac{\partial L_f^2 h_2}{\partial x_1} & \frac{\partial L_f^2 h_2}{\partial x_2} & \frac{\partial L_f^2 h_2}{\partial x_3} & \frac{\partial L_f^2 h_2}{\partial x_4} \end{pmatrix} \quad (23)$$

The computation of the corresponding determinant gives:

$$\begin{aligned} \Delta_2 &= \frac{\partial L_f^2 h_1}{\partial x_3}.\frac{\partial L_f^2 h_2}{\partial x_4} - \frac{\partial L_f^2 h_2}{\partial x_3}.\frac{\partial L_f^2 h_1}{\partial x_4} \\ &= b^2[-a^2 + am + 2k_t(-cos(x_3)x_1 \quad (24) \\ &- sin(x_3)x_2)]x_4 - 2b^2x_4^3 - b^2(a-m)\dot{x}_4 \end{aligned}$$

From equation (24) the observability loss for the considered output and only its first and second derivatives is $\Delta_2 = 0$. The associated manifold of unobservability is given by $\overline{\Omega} = \{x : \Delta_2(x) = 0 \text{ and } \Delta_1 = 0\}$.

Remark 4-3 In (24), at zero speed $x_4 = 0$, it is obvious that the SPMSM is locally weakly observable for $\dot{x}_4 \neq 0$. This is less restrictive than condition $\Delta_1 = 0$ given by (20).

Case 2: SPMSM at zero speed and acceleration

The problem now is to consider the particular case where $\dot{x}_4 = x_4 = 0$ (zero speed and acceleration), and to look if possible to recover the observability of SPMSM by using the higher order derivatives (greater than 2) of the output.

First: consider zero acceleration ($\dot{x}_4 = 0$)

The model of the SPMSM used in this case is given by (8)-(9) in the form of (10) where the function $f(x,u)$ is replaced by

$$f_0(x,u) = \begin{pmatrix} ax_1 + bx_4 sin(x_3) + cu_\alpha \\ ax_2 - bx_4 cos(x_3) + cu_\beta \\ x_4 \\ 0 \end{pmatrix}$$

and $h(x) = [x_1, x_2]^T$,

Consider now the vector of information generated by the output and its first, second and third derivatives:

$$O_3 = \begin{pmatrix} h_1 \\ h_2 \\ L_{f_0} h_1 \\ L_{f_0} h_2 \\ L_{f_0}^2 h_1 \\ L_{f_0}^2 h_2 \\ L_{f_0}^3 h_1 \\ L_{f_0}^3 h_2 \end{pmatrix} \quad (25)$$

The associated observability matrix is:

$$J_3 = \frac{\partial}{\partial x} O_3 = \begin{pmatrix} 1 & 0 & 0 & 0 \\ 0 & 1 & 0 & 0 \\ a & 0 & bx_4 cos(x_3) & bsin(x_3) \\ 0 & a & bx_4 sin(x_3) & -bcos(x_3) \\ a^2 & 0 & c_5 & d_5 \\ 0 & a^2 & c_6 & d_6 \\ a^3 & 0 & c_7 & d_7 \\ 0 & a^3 & c_8 & d_8 \end{pmatrix} \quad (26)$$

with

$$\begin{aligned} c_5 &= abx_4 cos(x_3) - bx_4^2 sin(x_3) \\ d_5 &= absin(x_3) + 2bx_4 cos(x_3) \\ c_6 &= abx_4 sin(x_3) + bx_4^2 cos(x_3) \\ d_6 &= -abcos(x_3) + 2bx_4 sin(x_3) \\ c_7 &= a^2 bcos(x_3)x_4 + (-absin(x_3)x_4 - bx_4^2 cos(x_3))x_4 \\ d_7 &= a^2 bsin(x_3) + abx_4 cos(x_3) - bx_4^2 sin(x_3) \\ &+ (abcos(x_3) - 2bx_4 sin(x_3))x_4 \\ c_8 &= a^2 bsin(x_3)x_4 + (abcos(x_3)x_4 - bx_4^2 sin(x_3))x_4 \\ d_8 &= -a^2 bcos(x_3) + abx_4 sin(x_3) + bx_4^2 cos(x_3) \\ &+ (absin(x_3) + 2bx_4 cos(x_3))x_4 \end{aligned}$$

Remark 4-4 In (26), at zero acceleration $\dot{x}_4 = 0$, it is obvious that the SPMSM is locally weakly observable for $x_4 \neq 0$.

Second: consider also $x_4 = 0$ (this corresponds to zero acceleration and speed)

In this case the observability matrix J_3 (26) becomes:

$$J_4 = \begin{pmatrix} 1 & 0 & 0 & 0 \\ 0 & 1 & 0 & 0 \\ a & 0 & 0 & bsin(x_3) \\ 0 & a & 0 & -bcos(x_3) \\ a^2 & 0 & 0 & absin(x_3) \\ 0 & a_2 & 0 & -abcos(x_3) \\ a^3 & 0 & 0 & a^2 bsin(x_3) \\ 0 & a^3 & 0 & -a^2 bcos(x_3) \end{pmatrix} \quad (27)$$

Remark 4-5

From the equation (27) a recurrence relation can be obtained

$$\frac{\partial}{\partial x} L_{f_0}^k h_i = a \frac{\partial}{\partial x} L_{f_0}^{k-1} h_i \mid_{x_4=0} \quad (28)$$

$k = 2,3, \quad i = 1,2.$ and can be generalized for higher derivatives.

Thus, the higher derivatives of the output greater than three do not recover additional information.

Remark 4-6

Equations (27) and (28) show that for the considered output (currents) and its derivatives at any order, the condition $\dot{x}_4 = x_4 = 0$ (zero speed and acceleration) generates a structural subset of indistinguishability $\{x: \quad x_4 = 0 \quad and \quad \dot{x}_4 = 0\}$.

A physical interpretation is related to have the Back Electromotive Forces (BEMFs) equal to zero at any time for $x_4 = \dot{x}_4 = 0$, then any information with respect to the SPMSM rotor position is in the dynamics of stator currents.

5 Robust MRAS Speed Observer

It has been shown in the last section that in the case of IPMSM, we have always the opportunity to find the observability even at zero speed operation. However, in the case of SPMSM, the observability is lost when the motor operates at zero speed and acceleration. In this section, a new MRAS speed observer with an improved zero-speed position estimation design is proposed for the SPMSM. The structure of the proposed MRAS speed observer is shown in Fig. 1. This structure is made up of a reference model, an adjustable model and an adaptation mechanism. In this structure the mechanical speed is considered slowly variable with respect to electrical dynamics. This assumption is a usual one for synchronous motor.

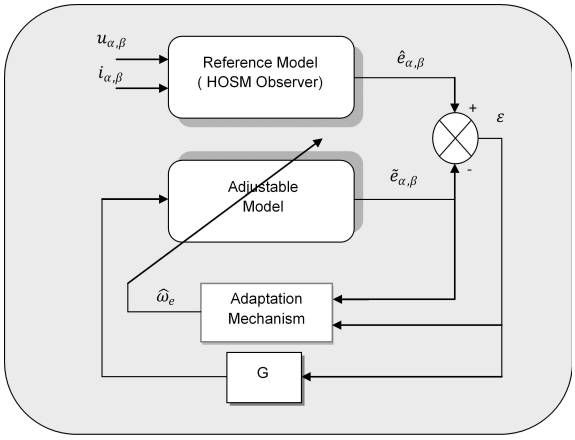

Figure 1: Structure of the MRAS Speed Observer based Sliding Mode

5.1 The reference model

The reference model consists in designing a second order sliding mode observer (Super Twisting Algorithm) which computes the reference BEMFs $\hat{e}_{\alpha,\beta} = [\hat{e}_\alpha \quad \hat{e}_\beta]^T$ using only measured stator currents and voltages. This reference model does not depend on the velocity.

The general form of the Super Twisting Algorithm (STA) is defined as follows [29]:

$$\begin{aligned} u(e_1) &= u_1 + \lambda_1 |e_1|^{\frac{1}{2}} sgn(e_1) \\ \dot{u}_1 &= \alpha_1 sgn(e_1) \end{aligned} \tag{29}$$

with $e_1 = x_1 - \hat{x}_1$, λ_1, $\alpha_1 > 0$ are the observer parameters, u_1 is the output of the observer, x_1 is the estimated variable and:

$$sgn(e_1) = \begin{cases} 1 & if \quad e_1 > 0 \\ -1 & if \quad e_1 < 0 \\ \in [-1 \quad 1] & if \quad e_1 = 0 \end{cases}$$

Let e_α and e_β be the BEMFs and $x = [i_\alpha \quad i_\beta]$. Consider only current dynamic equations of the SPMSM, we can write:

$$\begin{cases} \dot{x}_1 = ax_1 - be_\alpha + cu_\alpha \\ \dot{x}_2 = ax_2 - be_\beta + cu_\beta \end{cases} \tag{30}$$

with

$$\begin{cases} e_\alpha = -\omega_e \sin(\theta_e) \\ e_\beta = \omega_e \cos(\theta_e) \end{cases} \tag{31}$$

Let

$$[x_a \quad x_b] = -b[e_\alpha \quad e_\beta] \tag{32}$$

be the vector of unknown variables. Using (32), equation (30) becomes:

$$\begin{cases} \dot{x}_1 = ax_1 + x_a + cu_\alpha \\ \dot{x}_2 = ax_2 + x_b + cu_\beta \end{cases} \tag{33}$$

Currents and voltages are assumed to be measurable. Applying the STA (29) to system (33), we obtain systems (34) and (35):

$$\begin{cases} \dot{\hat{x}}_1 = \tilde{x}_a + ax_1 + cu_\alpha + \lambda_1 |e_1|^{\frac{1}{2}} sgn(e_1) \\ \dot{\tilde{x}}_a = \alpha_1 sgn(e_1) \end{cases} \tag{34}$$

$$\begin{cases} \dot{\hat{x}}_2 = \tilde{x}_b + ax_2 + cu_\beta + \lambda_2 |e_2|^{\frac{1}{2}} sgn(e_2) \\ \dot{\tilde{x}}_b = \alpha_2 sgn(e_2) \end{cases} \tag{35}$$

Where

$e_1 = x_1 - \hat{x}_1$, $e_2 = x_2 - \hat{x}_2$ and $\lambda_1, \lambda_2, \alpha_1, \alpha_2$ are positive constants that will be given later. $\tilde{x}_a$ and $\tilde{x}_b$ are the estimated values of the unknown variables x_a and x_b.

According to equations (33), (34) and (35), error dynamics of the observer are given by:

$$\begin{cases} \dot{e}_1 = e_a - \lambda_1 |e_1|^{\frac{1}{2}} sgn(e_1) \\ \dot{e}_a = f_1(x_b) - \alpha_1 sgn(e_1) \end{cases} \quad (36)$$

$$\begin{cases} \dot{e}_2 = e_b - \lambda_2 |e_2|^{\frac{1}{2}} sgn(e_2) \\ \dot{e}_b = f_2(x_a) - \alpha_2 sgn(e_2) \end{cases} \quad (37)$$

With $e_a = x_a - \tilde{x}_a$, $e_b = x_b - \tilde{x}_b$, $f_1(x_b) = \omega_e x_b$ and $f_2(x_a) = -\omega_e x_a$

Following the results proposed in [30] and [31] with respect to the super twisting algorithm (29) dedicated to the observer design given by equations (34) and (35), we set:

Corollary: For any initial conditions $x(0)$, $\hat{x}(0)$, there exists a choice of λ_i and α_i such that the observer state $\hat{x}$ converges in finite time to x, i.e. $\hat{x}_1 \longmapsto x_1$ and $\hat{x}_2 \longmapsto x_2$ then e_1, e_2, $\dot{e}_1$ and $\dot{e}_2$ converges to zero and by consequence $\tilde{x}_a \longmapsto x_a$ and $\tilde{x}_b \longmapsto x_b$.

Proof: Consider system (36). To show the convergence of $(\hat{x}_1, \tilde{x}_a)$ to (x_1, x_a) (ie., $(e_1, e_a) \rightarrow (0,0)$) let consider the system's dynamic $\ddot{e}_1$

$$\ddot{e}_1 = f_1(x_b) - \alpha_1 sign(e_1) - \frac{\lambda_1}{2} |e_1|^{-\frac{1}{2}} \dot{e}_1 \quad (38)$$

with $\frac{d|x|}{dt} = \dot{x} sign(x)$

Equation (38) leads to

$$\ddot{e}_1 \in \left[-f_1^+, f_1^+\right] - \alpha_1 sign(e_1) - \frac{\lambda_1}{2} |e_1|^{-\frac{1}{2}} \dot{e}_1 \quad (39)$$

where

$$f_1^+ = max(f_1(x_b)),$$

Figures 2 and 3 illustrate the finite time convergence behavior of the reference model. In what follows we will give the error trajectory for each quadrant in the worst cases.

First quadrant: $e_1 > 0$ and $\dot{e}_1 > 0$

Starting from point A of Fig. 2 the trajectory of $\dot{e}_1 = f(e_1)$ is in the first quadrant $e_1 \geq 0$ and $\dot{e}_1 \geq 0$. The rising trajectory is given by $\ddot{e}_1 = -(\alpha_1 - f_1^+)$

By choosing $\alpha_1 > f_1^+$ we ensure that $\ddot{e}_1 < 0$ and hence $\dot{e}_1$ decreases and tends towards the y-axis, corresponding to $\dot{e}_1 = 0$ (point B in Fig. 2).

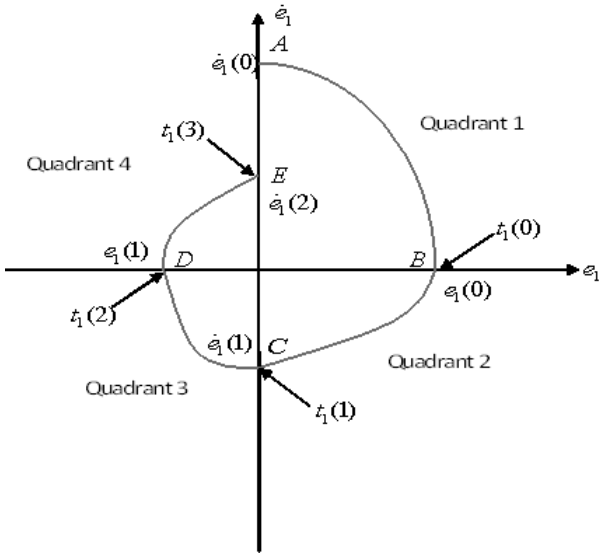

Figure 2: Finite time convergence behavior of the proposed observer : The majoring curve for the finite time convergence.

Let $e_1(0)$ be the intersection of this trajectory with $\dot{e}_1 = 0$; thus

$$e_1(0) = \frac{1}{2(\alpha_1 - f_1^+)} \dot{e}_1^2(0) \quad (40)$$

Then, the rising trajectory for $e_1 > 0$ and $\dot{e}_1 > 0$ can be given by the following expression:

$$\dot{e}_1^2 = 2(\alpha_1 - f_1^+)(e_1(0) - e_1) \quad (41)$$

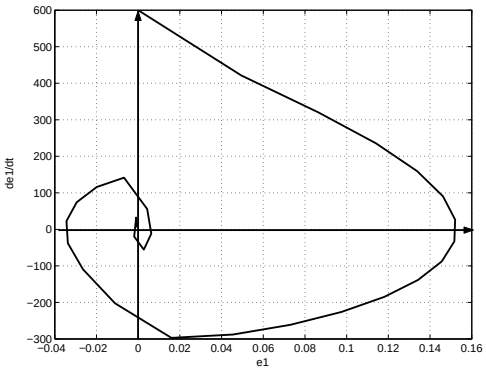

Figure 3: The trajectory $\dot{e}_1 = f(e_1)$: Finite time convergence.

Second quadrant: $e_1 > 0$ and $\dot{e}_1 < 0$

In this case, $\ddot{e}_1 = -f_1^+ - \alpha_1 sign(e_1) - \frac{\lambda_1}{2} |e_1|^{-\frac{1}{2}} \dot{e}_1$ becomes negative $(\ddot{e}_1 < 0)$ on making a good choice of α_1 which leads to $(\alpha_1 + f_1^+) > -\frac{\lambda_1}{2} |e_1|^{-\frac{1}{2}} \dot{e}_1$

So, the rising trajectories as illustrated in Fig. 2 are

given as $e_1 = e_1(0)$ with $0 \geq \dot{e}_1 \geq \frac{-2}{\lambda_1}(\alpha_1 + f_1^+)e_1^{1/2}$ and $\dot{e}_1 = \dot{e}_1(1) = \frac{-2}{\lambda_1}(\alpha_1 + f_1^+)e_1^{1/2}(0)$ with $\dot{e}_1 > \frac{-2}{\lambda_1}(\alpha_1 + f_1^+)e_1^{1/2}$ (where $\dot{e}_1(1)$ corresponds to the intersection of $\dot{e}_1 = \frac{-2}{\lambda_1}(\alpha_1 + f_1^+)e_1^{1/2}$ and $e_1 = e_1(0)$ (denoted by point C in Fig. 2)).
Hence, if $\frac{|\dot{e}_1(1)|}{|\dot{e}_1(0)|} < 1$ which means that $\lambda_1 > (\alpha_1 + f_1^+)\sqrt{\frac{2}{\alpha_1 - f_1^+}}$, we can state that

$$\alpha_1 > f_1^+ \quad and \quad \lambda_1 > (f_1^+ + \alpha_1)\sqrt{\frac{2}{\alpha_1 - f_1^+}} \quad (42)$$

are sufficient conditions guaranteeing the state convergence (i.e. the states $(e_1, \dot{e}_1)$ tend towards $e_1 = \dot{e}_1 = 0$ and in consequence the full convergence of $\sum_{i=0}^{\infty} |\dot{e}_1(i)|$).
Now we will consider the system (37). Following the same procedure, we can state that

$$\alpha_2 > f_2^+ \quad and \quad \lambda_2 > (f_2^+ + \alpha_2)\sqrt{\frac{2}{\alpha_2 - f_2^+}} \quad (43)$$

are sufficient conditions guaranteeing the state convergence (i.e. the states $(e_2, \dot{e}_2)$ tend towards $e_2 = \dot{e}_2 = 0$ and in consequence the full convergence of $\sum_{i=0}^{\infty} |\dot{e}_2(i)|$).
Where

$$f_2^+ = max(f_2(x_a)),$$

Now, in order to prove the finite time convergence, it is necessary to know the time passed in following the trajectory in each quadrant.
In the first quadrant, the rising trajectory is given by $\ddot{e}_1 = -(\alpha_1 - f_1^+)$. So, by integration, we can find that $\dot{e}_1 = -(\alpha_1 - f_1^+)t + cte$ with $cte = \dot{e}_1(0)$. Hence the necessary time for going from A to B is

$$t_1(0) = \frac{1}{(\alpha_1 - f_1^+)}\dot{e}_1(0) \quad (44)$$

In the second quadrant, we can find the rising trajectory leading to a much longer time. This is given by $\ddot{e}_1 = -f_1^+ - \alpha_1 - \frac{\lambda_1}{2}|e_1|^{-\frac{1}{2}}\dot{e}_1$. Then, as previously, we can write that $\dot{e}_1 = (-\alpha_1 - f_1^+)t - \lambda_1 e_1^{1/2} + cte$ with $cte = \lambda_1 e_1^{1/2}(0)$ because at B we have $t = 0$ and $\dot{e}_1 = 0$. Now in C we have $\dot{e}_1(1) = (-\alpha_1 - f_1^+)t_1(1) + \lambda_1 e_1^{1/2}(0)$; then the necessary time for going from B to C is $t_1(1) = \frac{-\dot{e}_1(1) + \lambda_1 e_1^{1/2}(0)}{\alpha_1 + f_1^+}$ which can be expressed as a function of $\dot{e}_1(0)$ as:

$$t_1(1) = \frac{2(\alpha_1 + f_1^+) + \lambda_1^2}{\lambda_1(\alpha_1 + f_1^+)\sqrt{2(\alpha_1 - f_1^+)}}\dot{e}_1(0) \quad (45)$$

Following the same procedure and using the property of symmetry of the first and the third quadrant, we can find the time for going from C to D which can be given by $t_1(2) = \frac{-1}{(\alpha_1 - f_1^+)}\dot{e}_1(1)$, and expressed also as function of $\dot{e}_1(0)$ as

$$t_1(2) = \frac{2}{\lambda_1\sqrt{2(\alpha_1 - f_1^+)}}\dot{e}_1(0) \quad (46)$$

and for the second and fourth quadrants, the time for going from D to E is $t_1(3) = \frac{\dot{e}_1(2) + \lambda_1|e_1(1)|^{1/2}}{\alpha_1 - f_1^+}$; since $\dot{e}_1(2) = \frac{2(\alpha_1 - f_1^+)}{\lambda_1^2}\sqrt{\frac{\alpha_1 + f_1^+}{\alpha_1 - f_1^+}}\dot{e}_1(0)$ and $|e_1(1)|^{1/2} = \frac{1}{\lambda_1}\sqrt{\frac{\alpha_1 + f_1^+}{\alpha_1 - f_1^+}}\dot{e}_1(0)$, one easily obtains

$$t_1(3) = \frac{2(\alpha_1 - f_1^+) + \lambda_1^2}{\lambda_1^2(\alpha_1 - f_1^+)}\sqrt{\frac{\alpha_1 + f_1^+}{\alpha_1 - f_1^+}}\dot{e}_1(0) \quad (47)$$

Let $T_d(1)$ be the necessary time interval for going from A to E; then

$$T_d(1) = t_1(0) + t_1(1) + t_1(2) + t_1(3) = \bar{K}\dot{e}_1(0) \quad (48)$$

where

$$\begin{aligned} \bar{K} &= \frac{1}{(\alpha_1 - f_1^+)} + \frac{2(\alpha_1 + f_1^+) + \lambda_1^2}{\lambda_1(\alpha_1 + f_1^+)\sqrt{2(\alpha_1 - f_1^+)}} \quad (49) \\ &+ \frac{2}{\lambda_1\sqrt{2(\alpha_1 - f_1^+)}} + \frac{2(\alpha_1 - f_1^+) + \lambda_1^2}{\lambda_1^2(\alpha_1 - f_1^+)}\sqrt{\frac{\alpha_1 + f_1^+}{\alpha_1 - f_1^+}} \end{aligned}$$

and thus the convergence time for this step can be, in the worst case, given as

$$\begin{aligned} T_1 &= \sum_{i=1}^{\infty} T_d(i) = \bar{K}\dot{e}_1(0) + \bar{K}W\dot{e}_1(0) + \bar{K}W^2\dot{e}_1(0) \\ &+ \bar{K}W^3\dot{e}_1(0) + ... \quad (50) \end{aligned}$$

which gives

$$T_1 = \frac{1}{1 - W}\bar{K}\dot{e}_1(0)$$

With $W = \frac{2(\alpha_1 - f_1^+)}{\lambda_1^2}\sqrt{\frac{\alpha_1 + f_1^+}{\alpha_1 - f_1^+}} < 1$ and where λ_1 is given by (42), and by consequence, we can finally

conclude on the finite time convergence of $(\hat{x}_1, \tilde{x}_a)$ towards (x_1, x_a).
The same procedure is followed to demonstrate the finite time convergence of $(\hat{x}_2, \tilde{x}_b)$ towards (x_2, x_b).

Having $\tilde{x}_a$ and $\tilde{x}_b$ we can easily deduce the estimated BEMFs $\hat{e}_{\alpha,\beta}$ using (32).

5.2 The adjustable model

The adjustable model is tunable by the estimated velocity and it computes the estimated BEMFs $\tilde{e}_{\alpha,\beta} = [\tilde{e}_\alpha \quad \tilde{e}_\beta]^T$ from the following equation:

$$\dot{\tilde{e}}_{\alpha,\beta} = \hat{\omega}_e J \tilde{e}_{\alpha,\beta} + G(\tilde{e}_{\alpha,\beta} - \hat{e}_{\alpha,\beta}) \quad (51)$$

where $\hat{\omega}_e$ is the estimated velocity (the output of the MRAS observer (show fig. 1)) and

$$J = \begin{pmatrix} 0 & -1 \\ 1 & 0 \end{pmatrix} \quad (52)$$

For convergence, a feedback loop is introduced and the feedback gain is:

$$G = g \begin{pmatrix} 1 & 0 \\ 0 & 1 \end{pmatrix} \quad (53)$$

where g is a positive constant.

5.3 The adaptation mechanism

If the velocity estimation error exist, it will lead to the estimated BEMFs estimation error :

$$\varepsilon = \hat{e}_{\alpha,\beta} - \tilde{e}_{\alpha,\beta} \quad (54)$$

Then, this error together with the estimation model's output $\tilde{e}_{\alpha,\beta}$ is used to construct the manifold S as :

$$S = \varepsilon^T J \tilde{e}_{\alpha,\beta} \quad (55)$$

The estimated velocity is :

$$\hat{\omega}_e = M sgn(S) \quad (56)$$

Note that the speed estimate is a discontinuous function of the manifold and M is a positive constant. The BEMFs $\hat{e}_{\alpha,\beta}$ computed by the reference model will converge in finite time T_1 to $e_{\alpha,\beta}$. After this time $(t > T_1)$, the BEMFs used in the reference model are also satisfied the following equation:

$$\dot{\hat{e}}_{\alpha,\beta} = \omega_e J \hat{e}_{\alpha,\beta} \quad (57)$$

To show that the sliding mode can be enforced in the manifold $S = 0$, we need to show that there exist M sufficiently high such that the manifold is attractive:

$$S\dot{S} < 0 \quad (58)$$

After differentiating (55) and replacing the derivative of the BEMFs from (51) and (57), the following expression is obtained:

$$\begin{aligned} \dot{S} &= f(\omega_e, \hat{e}_{\alpha,\beta}, \tilde{e}_{\alpha,\beta}) \\ &- M(\tilde{e}^T_{\alpha,\beta} \hat{e}_{\alpha,\beta}) sgn(S) \end{aligned} \quad (59)$$

where f is a function of the reference and estimated BEMFs and speed. Since this term is greater than zero when the motor is exited and f has a positive upper value, it's clear from (59) that sufficiently high M can be selected such that condition (58) is fulfilled. Thus, sliding mode is enforced in the manifold S and after sliding mode begins, we have $S = 0$. The boundary layer method described in [25] is used to find the equivalent control $\omega_{e,eq}$. Once sliding mode occurs, we can also assume $\dot{S} = 0$ along with $S = 0$. The expression of the equivalent control becomes:

$$\omega_{e,eq}[\tilde{e}^T_{\alpha,\beta} \hat{e}_{\alpha,\beta}] = \omega_e[\tilde{e}^T_{\alpha,\beta} \hat{e}_{\alpha,\beta}] + g\varepsilon^T J \tilde{e}_{\alpha,\beta} \quad (60)$$

From (60) when the manifold converge to zero ($S = \varepsilon^T J \tilde{e}_{\alpha,\beta} = 0$), the equivalent speed tends to the real speed. The equivalent speed represents the low-frequency component of the discontinuous term (56). Thus, while the high-frequency switching function is fed into the observer, its low-frequency component can be obtained by Low-Pass Filtering (LPF) and represents the speed estimate.

5.4 The Rotor Position Estimation Design

The estimated rotor position is obtained simply from the phase of the estimated BEMFs as follows:

$$\hat{\theta}_e = \arctan 2(\frac{-\hat{e}_\alpha}{\hat{e}_\beta}) \quad (61)$$

However, it is shown in section four that the SPMSM is not observable at zero speed. To overcome this problem, un Estimator/Observer swapping system is proposed to ensure position estimation in all speed range and to overcome position observability problems at very low frequencies. The estimator is obtained by integrating the estimated speed as:

$$\hat{\theta}_e = \int_0^t \hat{\omega}_e dt + cte \quad (62)$$

The initial value of the estimated position ($\hat{\theta}_e(0) = cte$) is equal to the last value computed by the observer

(61) before swapping to the estimator. Thus, since the speed is always observable, there is no problem of observability using this position estimator. So, the position is equal to the observer (61) when the motor operate at high frequencies and swap to the estimator (62) since the speed becomes less than a defined very low value.

6 Simulation Results

The used motor in the simulation testing is a three-phase SPMSM. The specifications and parameters are listed in Table 1. Parameters of the MRAS observer are given in Table 2. The observer is tested in open loop. Using current and voltage signals, the BEMFs are estimated using the proposed SOSM observer which is used as the reference model in the MRAS structure. This observer does not depend on the speed. The adjustable model is tunable by the estimated speed and it is implemented using equation (51) (the output of the MRAS observer ($\hat{\omega}_e$) is used as a feedback to adjust the adjustable model as shown in Fig. 1).

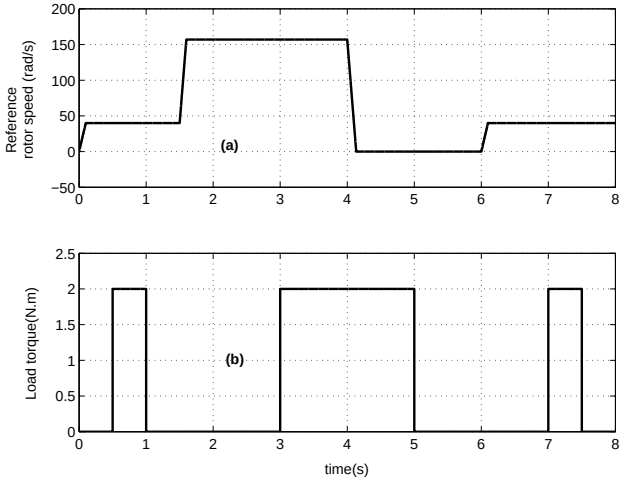

Figure 4: Benchmark trajectories: (a) Reference rotor speed (rad/s), (b) Load torque (N.m)

Dedicated Benchmark. The proposed observer is tested to the benchmark trajectories [35] presented in Fig. 4. In this benchmark, two reference trajectories are defined: The reference rotor speed (Fig. 4(a)) and the load torque (Fig. 4(b)). Initially, the motor is started to run from zero and increase to 40 rad/s and still constant until t=1.5s. The load torque is applied at t=0.5s and removed at t=1s. This first phase permit to test and evaluate the performance and the robustness of the observer at low frequencies with application of the load torque. At t=1.5s, the motor is accelerated until high frequency (157 rad/s). Then, the load torque is

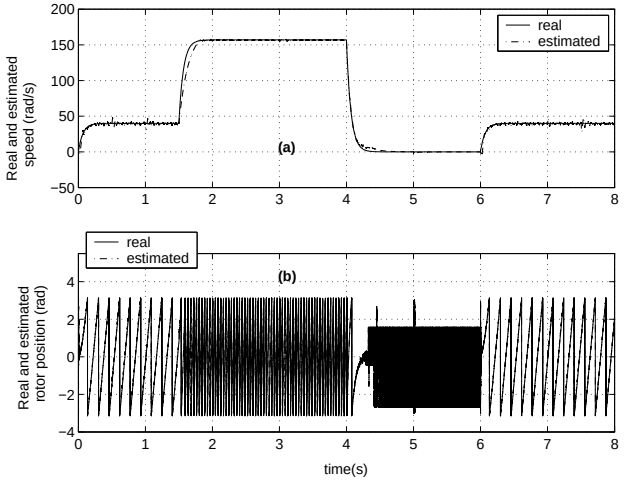

Figure 5: Nominal Case: (a) Real and estimated rotor speed (rad/s), (b) Real and estimated rotor position (rad)

applied again at t=3s. This second phase permit to test the robustness of the observer at high frequency operating conditions. After that, the motor is decelerated to 0rad/s and still constant (zero speed and acceleration) until t=6s. This last phase permit to illustrate the observability problems of the SPMSM at zero speed and acceleration. Finally, the motor is controlled out of the unobservable conditions. So the motor is tested at nominal case (Fig. 5 and 6). Robustness to internal disturbances is then tested by variation of +50% of stator resistance (Fig. 7), +15% of stator inductance (Fig. 8) and +15% of rotor flux (Fig. 9).

Speed Estimation. From these tests, we remark that the estimated speed mach the real one with very small steady-state error and good dynamics. The proposed observer is of high accuracy and robustness against internal disturbances (parameter variations) and external disturbances (load torque). Nevertheless an error occurs at fast changed speed time (for example in Fig. 5 at t=1.6 s) because in this case the speed is not slowly variable compared to the electrical dynamic. Obviously this behavior is not a physically one. It is done only to show the limit performances of the proposed control.

Rotor position Estimation. For rotor position estimation, two tests are carried out. In the first test, we use only the observer (Fig. 5). Fig. 5(b) shows the estimated position which reach the real one with good accuracy and robustness. However, at zero speed and acceleration, the rotor position is not observable. In the second test, we use the Estimator/Observer swapping system (Fig. 6, Fig. 7, Fig. 8 and Fig. 9). Thus, in these figures, we show that the rotor position can be obtained at all range of frequencies. However, in

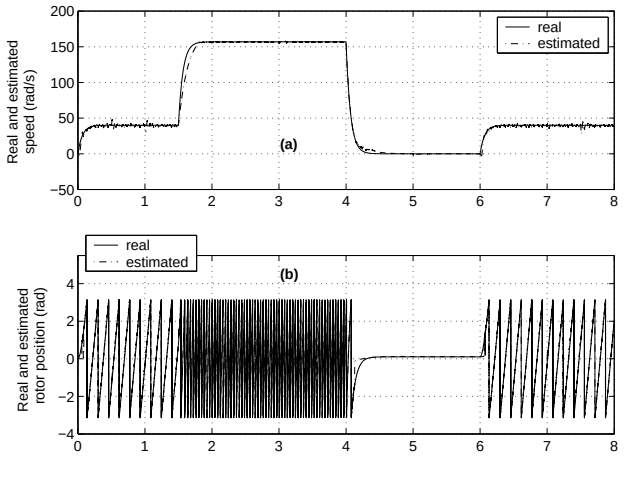

Figure 6: Estimator/Observer Swapping: Nominal Case: (a) Real and estimated rotor speed (rad/s), (b) Real and estimated rotor position (rad)

the unobservable region, we remark in Fig. 6 that the estimated position is sensitive only to stator resistance variation. This is due to the use of the estimator in this region and not the observer.

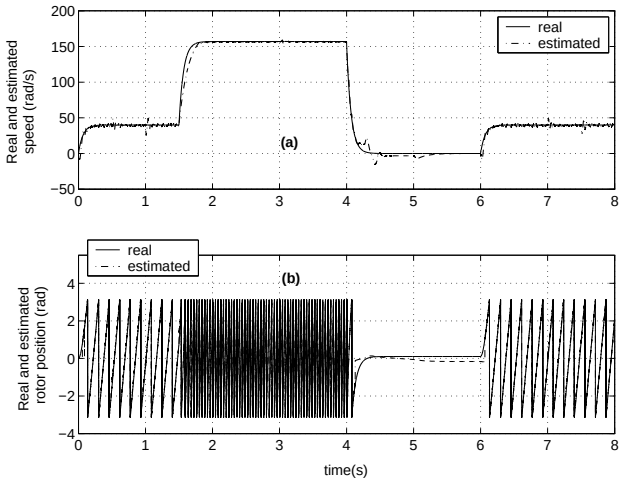

Figure 7: Estimator/Observer Swapping: +50% variation of stator resistance: (a) Real and estimated rotor speed (rad/s), (b) Real and estimated rotor position (rad)

7 Conclusion

In this paper, the observability analysis of both the SPMSM and the IPMSM has been presented and discussed at different operating conditions. A necessary and sufficient observability condition has been presented. It has been shown that in the case of IPMSM,

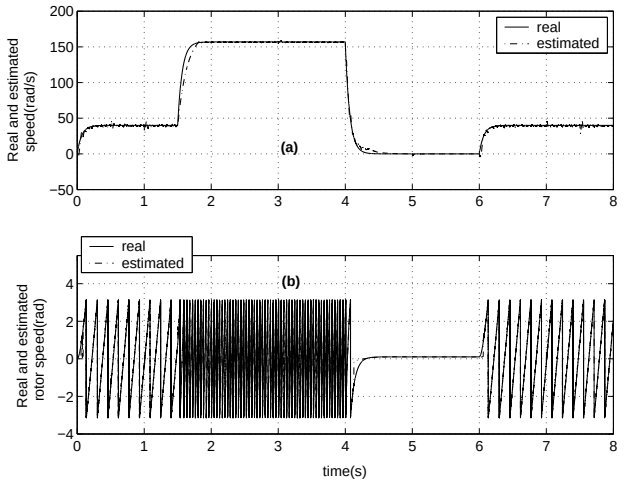

Figure 8: Estimator/Observer Swapping: +15% variation of stator inductance: (a) Real and estimated rotor speed (rad/s), (b) Real and estimated rotor position (rad)

we have always the opportunity to find the observability even at zero speed operation. However, in the case of SPMSM, the observability is lost when the motor operates at zero speed and acceleration. Furthermore, a new robust MRAS scheme based sliding mode techniques is proposed for high accuracy and robustness rotor speed estimation of a SPMSM. The stability of the proposed MRAS system has been studied and discussed. High performance estimation of the rotor position has been obtained using an Estimator/Observer swapping system and permit to overcome the problem of observability at low speed. Selected simulation results has been presented to illustrate the performance and the robustness of the proposed speed and position estimations design.

Acknowledgements: The authors thank Doctor Malek GHANES and Professor Jean Pierre BARBOT for their helpful insight and support.

References:

[1] S. Bolognani, L. Tubiana and M. Zigliotto, Extented Kalman Filter tuning in sensor-less PMSM drives, *IEEE trans. Ind. Appl, vol. 39, no. 6*, 2003, pp. 1741-1747.

[2] J. Solsona, M. I. Valla and C. Muravchik, A non linear reduced order observer for permanent magnet synchronous motors, *IEEE trans. Ind. Electr., vol. 43, no.4*, 1996, pp. 492-497.

[3] K. Y. Lian, C. H. Chiang and H. W. Tu, LMI-based sensor-less control of permanent magnet

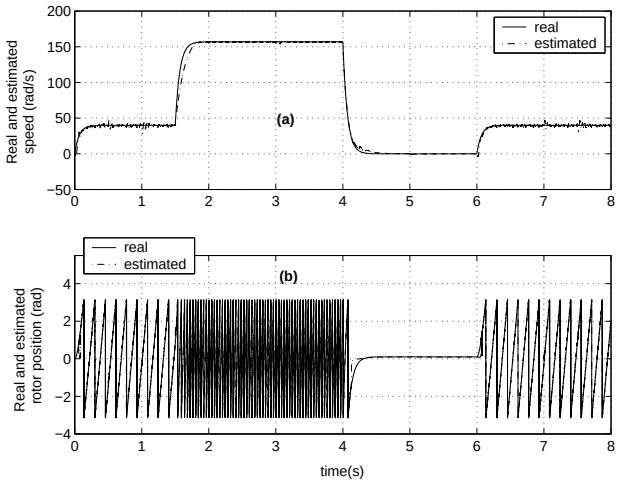

Figure 9: Estimator/Observer Swapping: +15% variation of rotor flux: (a) Real and estimated rotor speed (rad/s), (b) Real and estimated rotor position (rad)

synchronous motors, *IEEE trans. Ind. Elect.* , *vol. 54, no. 5,* 2007, pp. 2769-2778.

[4] A. Piippo, J. Salomaki and J. Luomi, Signal injection in sensor-less PMSM drives equipped with inverter output filter, *IEEE PCC'07., 2007,* pp. 1105-1110.

[5] J. H. Jang, S. K. Sul, J. I. Ha et al, Sensor-less drive of surface-mounted permanent magnet motor by high frequency signal injection based on magnetic saliency, *IEEE Trans. Industry Appl., vol. 39, no 4,* 2003, pp. 1031-1039.

[6] K. Paponpen and M. Konghirun, An improved sliding mode observer for speed sensor-less vector control drive of PMSM, *IEEE IPEMC'06, vol. 2,* 2006. pp. 1-5.

[7] C. S. Li and M. Elbuluk, A Robust Sliding Mode Observer for permanent magnet synchronous motor drives, *IEEE IECON'02, vol. 2,* 2002, pp. 1014-1019.

[8] C. Silva, G. M. Asher and M. Sumner, Hybrid rotor position observer for wide speed range sensor-less PM motor drives including zero speed, *IEEE trans. Ind. Elect., vol .53, no. 2,* 2006, pp. 373-378.

[9] K. L. Kang, J. M. Kim, K. B. Hwang et al, Sensor-less Control of PMSM in high speed range with iterative sliding mode observer, *IEEE APEC, vol. 2,* 2004, pp. 1111-1116

[10] S. Nakashima, Y. Inagaki, I. Miki, Sensor-less initial rotor position estimation of surface permanent magnet synchronous motor, *IEEE Trans. Ind. Appl., vol. 36, No. 6,* 2000, pp. 1598-1603.

[11] R. Wu, G. R. Slemon, A permanent magnet motor drive without a shaft sensor, Industry Applications Society Annual Meeting, 1990, 7-12 october, pp. 553-558.

[12] M. Ghanes, J. De Leon and A. Glumineau, Observability Study and Observer-Based Interconnected Form for sensor-less Induction Motor, *IEEE conf. on Decis. and cont.,* 2006, pp. 1240-1245.

[13] S. Ibarra-Rojas, J. Moreno and G. Espinosa-Prez, Global observability analysis of sensorless induction motors, *Automatica vol 40,* 2004, pp. 1079-1085.

[14] X. Junfeng, W. Fengyan, X, Shaofeng, X. Jianping, F. Jianghua, A New Control method for Permanent Magnet Synchronous Machines with Observer, *35th annual IEEE Pow. Elect. Specialists Conf, Achan, Germany,* 2004, pp. 1400-1408.

[15] P. Vaclavec and P. Blaha, Synchronous Machine Drive Observability Analysis for sensorless Control Design, *16th IEEE Int. Conf. on Cont. and Appl., oct.* 2007, pp. 1113-1117.

[16] P. Vaclavec and P. Blaha, Synchronous Machine Drive Observability Analysis and sensorless Control Design, *2nd IEEE Int. Conf. on Pow. and Energ.,* dec. 2008, pp. 265-270.

[17] D. Zaltni, M. Ghanes and J.P. Barbot, Super Twisting Observer for Sensor-less Control of PMSM, *In proc. of the International IASTED conferences, Control and Applications,* 13-15 July, 2009, Cambridge, United Kingdom, pp. 129-135.

[18] D. Zaltni, M. Ghanes and J.P. Barbot, Observability Analysis of PMSM, *In proc. of IEEE Int. conf., Sign. Circ. and Syst.,* 6-8 Novem, 2009, Djerba, Tunisia, pp. 1-6.

[19] C. Schauder, Adaptative Speed Identification for Vector Control of Induction Motors without Rotational Transducers, *IEEE trans. Ind. Appl.,* Vol. 28, No. 5, 1992, pp. 2769-2778.

[20] S. Maiti, C. Chakraborty, Y. Hori and M. C. Ta, Model Reference Adaptative Controller-Based Rotor Resistance and Speed Estimation Techniques for Vector Controlled Induction Motor Drive Utilizing Reactive Power, *IEEE trans. Ind. Elect.,* Vol. 55, No. 2, 2008, pp. 594-601.

[21] C. M. Ta, T. Uchida and Y. Hori, MRAS-based Speed Sensorless Control for Indution Motor Drives using Instantaneous Reactive Power, *Proc. 27th IEEE Conf. on Ind. Elect. Soc.*, 2001, pp. 1417-1422.

[22] Y. S. Kim, S. K. Kim and Y. A. Kwon, MRAS based Sensorless Control of Permanent Magnet Synchronous Motor, *SICE Annual Conf., Fukui, August 4-6, 2003, pp. 1632-1638.*

[23] M. M. Kojabadi and C. Liuchen, Sensorless PMSM drive with MRAS-based adaptive speed estimator, *Proc. 37th IEEE Spec. conf. on Pow. Elect., 18-22 June 2006, Jeju*, 2006, pp. 1-5.

[24] D. Zaltni and M.N. Abdelkrim, "Robust MRAS Speed Observer and an Improved Zero-speed Position Estimation Design for SPMSM," In Proc. 6th WSEAS Int. Conf. on Dynam. Syst. and Cont. (CONTROL'10), 3-6 May, 2010, Sousse, Tunisia, pp. 202-210.

[25] V. Utkin, J. Guldner and J. Shi, *Sliding mode control in electromechanical systems, London*: 1st Edition, Taylor et Francis, 1999.

[26] L. Sbita, D. Zaltni and M. N. Abdelkrim, Adaptative Variable Structure Control for an Online Tuning Direct Vector Controlled induction motor drive, *Int. J. Appl. Sienc. Vol. 7, No. 21,* , 2007, pp. 3177-3186.

[27] M. Ghanes and G. Zheng, On Sensorless Induction Motor Drives: Sliding-Mode Observer and Output Feedback Controller, IEEE Transactions on Industrial Electronics (TIE), Vol.56, Sept., 2009, pp. 3404-3413

[28] G. Bartolini, A. Ferrara and E. Usani, Chattering Avoidance by Second-Order Sliding Mode Control, *IEEE trans. Autom. Cont.*, Vol. 43, No. 2, 1998, pp. 241-246.

[29] L. Fridman, A. Levant, Sliding modes of higher order as a natural phenomenon in control theory. In Robust control via variable structure and Lyapunov techniques, Lecture notes in control and information Science 217. F. Garofalo, L. Glielmo Ed. Springer Verlag London, 1996, pp. 107-133.

[30] A. Levant, Robust exact differentiation via sliding mode technique, *Automatica*, Vol. 34, No. 3, 1998, pp. 379-384.

[31] W. Perruquetti, J. P. Barbot, *Sliding mode Control in engineering*, New York: Marcel Dekker, 2002.

[32] Z. Chen, M. Tomita, S. Doki and S. Okuma, An Extended Electromotive Force Model for Sensor-less Control of Interior Permanent-Magnet Synchronous Motors, *IEEE trans. Ind. Elect.*, vol. 50, no. 2, Avr. 2003, pp. 288-295.

[33] R. Hermann, A. J. Krener, Non linear Controllability and Observability, *IEEE Trans. Autom. Cont.*, vol. AC-22, No. 5, Oct. 1977, pp. 728-740.

[34] J. P. Gauthier, and G. Bornard, Observability for any u(t) of a class of nonlinear systems. *IEEE Transactions on Automatic Control*, Vol 26 n4, 1981, pp. 922-926.

[35] A. Glumineau, R. Boiliveau (IRCcyN), L. Loron (IREENA), "www.irccyn.ec-nantes.fr/hebergement/bancEssai", 2008.

Table 1: PMSM characteristics

Rated Power P_n	$1.7kW$
Rated speed ω_n	$157rad.s^{-1}$
Rated voltage U_n	$380V$
Rated current I_n	$3.8A$
Number of pole pairs P	3
Stator inductance L_0	0.027H
Stator resistance R	3.3 Ω
Rotor flux ϕ_m	0.341
Rotor inertia J	$0.0026kg.m^2$
Viscous friction f_v	$0.0034kg.m^2.s^{-1}$

Table 2: Parameters of the Observer.

α_1	5.10^5
λ_1	580
α_2	5.10^5
λ_2	800
g	100
M	1500